Optimization of Electromechanical Properties of Piezoelectric Nanocomposite Elastomers

Evan Bird[1] and David Wood[1]
BYU Mechanical Engineering, Provo, UT

Nanocomposite elastomers, including highly flexible strain gauges and foam, have been shown to exhibit a piezo-response, or change in electrical impedance, under mechanical strain. Both classes of sensors are comprised of an elastomer matrix (typically silicone for strain gauges and polyurethane or latex for foam) mixed with conductive nanofillers including nickel-coated carbon fiber and nickel powder. Though these sensors are used for different applications, their piezoresistive responses can be optimized with respect to the same variables. An optimal piezo-response for each sensor is defined by a maximum range of output resistance registered during strain. Parameters of both nanocomposites that similarly affect their piezo-responses include sensor size (length, width, height) and volume fraction of the conductive filler. Since the relationships between these and the resistance values of interest are similar between both sensors, they are selected to optimize as design variables. The optimal width, thickness, and filler volume fraction for a piezoresistive nanocomposite is found deterministically and accounting for uncertainty. Results show that small sensors with a high volume fraction of conductive fillers yield optimal resistance ranges at a given strain.

I. Introduction

Elastomer-based nanocomposites are useful in a variety of piezoresistive sensing applications. This class of sensors exhibits a piezo-response, or change in electromechanical impedance, when mechanically strained in tension. It is because of this response that they have recently been studied as a novel approach to large strain sensing [1]. Though each exploits this same physical phenomenon, each can be classified by one of two groups: tension or compression sensors. Tension can be sensed by embedding nickel nanofillers in a silicone matrix to make a flexible and inexpensive strain gauge. Embedding the same conductive nanofillers in a polyurethane of latex foam matrix creates a sensor that can detect compressive strains.

These sensors show promise in applications including wearable sensors, smart fabrics, mattresses, and pressure mats, among others. Previous attempts to model the electromechanical response of similar sensors have been performed; however, sensors were only included in a study of a larger actuator-driven mechanical system and not investigated explicitly [2-4]. Similar studies have been conducted using thin film metallic strain gauges [5], but their results cannot be directly related to polymer based composites. Metallic thin film strain gauges were shown to exhibit high accuracy, but were not able to sense strains in excess of 5% due to the relatively low flexibility of their metal-foil designs and metallic matrices. This work attempts to optimize an elastomeric nanocomposite sensor's electrical response with respect to its physical size and composition. It also finds the effective range of strains that a specific polymer composite sensor can measure. This will help to more deeply understand the sensor's piezoresistive behavior and serve as a proof of concept for large strain sensing composites.

II. Methodology

The coupling of the electrical and elastic properties of nanocomposite sensors is derived from basic theory in electronics and continuum mechanics [6]. Each class of sensor can be modeled as a simple beam, where one dimension is much larger than the other two, to simplify the governing equations. This assumption yields a simplified one-dimensional model rather than a more accurate but highly complex higher dimensional model that is dependent on microstructural electron interactions. To couple the 1D equation for strain displacement in the long direction, u_1, with the sensing material's electrical properties, we start with the definition of electrical resistance:

$$R = \rho' \left(\frac{L}{A}\right) \tag{1}$$

where ρ' is the material's resistivity, L is the length of the element, and A is the cross-sectional area. Each sensor is also assumed to be isotropic and infinitely stiff in the two non-strained directions ($\nu = 0.5$), which simplifies the 1D

[1] Graduate Student, Department of Mechanical Engineering, 435 Crabtree Building, Provo, UT 84602

equation while still providing an accurate representation of the system. As the sensor is strained its resistance increases and we can derive a model of its change in resistance, which becomes the objective to be maximized. Noting that the dimension terms in Eq. 1 are only functions of the strain, ε_{11}, the change in electrical resistance takes the form:

$$\Delta R = \rho' \left(\frac{u_1}{\Delta A}\right) = \frac{\rho' u_1}{L_2\, L_3\, \nu^2\, \varepsilon_{11}^2}) \tag{2}$$

An equation modeling the desired displacement is used as the variable u_1. A constant applied force with no damping displacement was used in our calculations:

$$u_1 = ax^2 + bx + c \tag{3}$$

where x is the half length of the strained sensor. For the following simulations 12, 40, and 0 were used for a, b, and c, respectively. A correlation between resistivity and the volume fraction of filler in the sensor was experimentally found and fit to a curve. This curve was found by taking experimental data found in Ref. [7] and fitting a modified log-normal curve to create the following correlation:

$$\rho' = \frac{xde^{-\frac{log(\frac{\varepsilon_{11}}{c})^2}{2a^2}}}{a\frac{\varepsilon_{11}}{c}\sqrt{2\pi}} \tag{4}$$

where the parameters a, c, and d are:

$$a = 1766.3{V_f}^2 - 192.1V_f + 6.2$$
$$c = 504.36{V_f}^2 - 52.75V_f + 1.5$$
$$d = 0.8{V_f}^{11.28}$$

Three experiments were performed in Ref. 7 to find the best fit model each of the parameters of the log-normal equation with respect to V_f. Combining Eqs. 2-4 yields the final objective function to be optimized:

$$\Delta R = \left(\frac{x\left(0.8{V_f}^{11.28}\right) e^{\left(-\frac{log(\frac{\varepsilon_{11}}{(504.36{V_f}^2-52.75V_f+1.5)})^2}{2(1766.3{V_f}^2-192.1V_f+6.2)^2}\right)}}{(1766.3{V_f}^2-192.1V_f+6.2)\frac{\varepsilon_{11}}{(504.36{V_f}^2-52.75V_f+1.5)}\sqrt{2\pi}} \right) \frac{12x^2+40x}{L_2 L_3 \nu^2 \varepsilon_{11}^2} \tag{5}$$

This model is an approximation of the exhibited responses of the composites and does not necessarily reflect the actual model. Addition governing equations, among them the rod theories of continuum mechanics, would have to be addressed and confirm that this model agrees with those governing equations.

Multiple constraints were enforced in this optimization to ensure that the optimized solution yielded manufacturable, practical, and desirable values for the design variables.

$$5 \le L_3 \le 12\ mm \tag{6}$$
$$1 \le L_2 \le 5\ mm \tag{7}$$
$$0 \le v_f \le 0.4 \tag{8}$$

The variables of x and ν were treated as constant parameters (with values of 70 mm and 0.5, respectively), while the optimization iterated ε_{11} over the range of possible strain values of 1-40%.

As the objective and constraints currently stand, we expect a high sensitivity of sensor thickness and piezoelectric coefficient per unit output. Other dimensions will correlate, but won't demonstrate such great sensitivity as the other design variables. This may lead to an ill-conditioned design space in two dimensions, and pose unforeseen issues in finding the absolute minimum of the objective function. To fix this, design variables, constraints, and objective, were all scaled to the order of one. At the conclusion of the optimization, design variables were scaled back to their original magnitude and the objective function recalculated to find the properly scaled optimal value.

III. Results and Discussion

A. Deterministic Optimization

A one hundred agent Particle Swarm simulation was used to test the objective function's conditioning with respect to each design variable. The function was found to be well behaved in all dimensions and optimizing the objective at various degrees of strain was easily implemented with a gradient-based constrained optimization tool (MATLAB's "fmincon" function using the interior-point solver). Fig. 1 shows the optimized values of ΔR as a function of strain. Though the optimization was performed over the entire elastic range of a strain gauge (0-0.4 strain), Fig. 1 shows that the piezoresistive response becomes very low at higher strains. Changes in resistance of less than 100 Ω are difficult to measure in strain gauges that already have unstrained resistances on the order of 10 kΩ. As such, this optimization shows that the sensing ability of nickel-silicone strain gauges becomes ineffective in response to strains greater than $\epsilon = 0.15$.

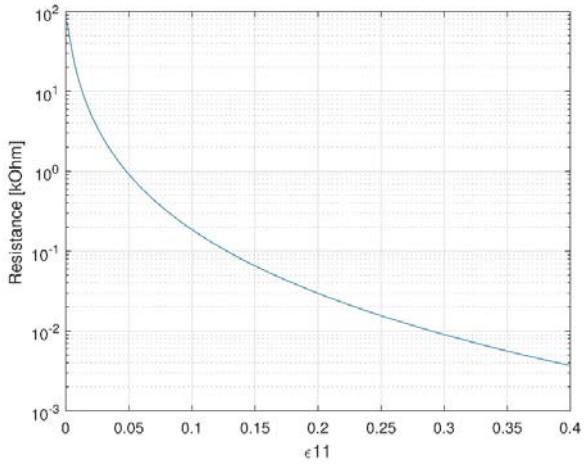

Figure 1. Optimized values of ΔR as a function of strain, for strains in the range of 1-40%.

The optimal design variable values were the same for all iterations of strain. The optimal values were $V_f = 0.4$, $L_2 = 0.001$ mm, and $L_3 = 0.005$. These results, however, are not entirely indicative of the experimental results future experiments are expected to yield. Because many of the material properties and displacement curves were experimentally measured and correlations were made with a least-squared regression, there is significant uncertainty in those parameters that can adversely affect the objective value. Material properties and correlations were treated as deterministic values in the previous analysis. Also, the deterministic optimization yielded optimal design variables that lie directly on the constraints: width and thickness on the lower bound, and volume fraction of filler on the upper bound. This can lead to designs that do not satisfy each half of the time. Therefore, inherent variability in the manufacturing procedure may generate design variables that could produce unreliable strain gauges (ones that are too difficult or costly to manufacture).

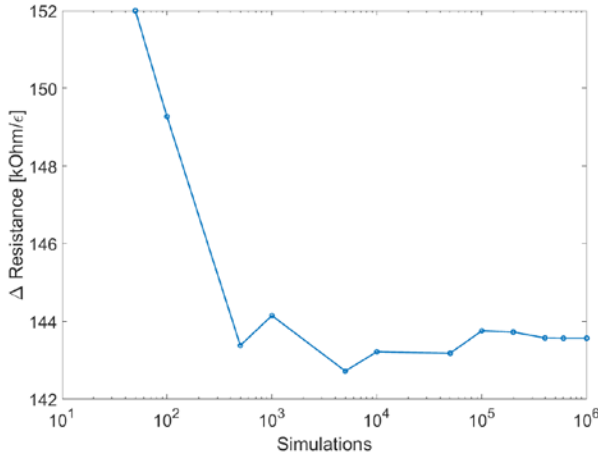

Figure 2. Monte Carlo convergence plot, showing changes in resistance at $\epsilon = 0.15$.

Each of these issues is addressed in the following sections by performing a Monte Carlo simulation and transmitted variance analysis on the previous design.

B. Monte Carlo Simulation

Using the parameter values used in the previous analysis as mean values, standard deviations (Table 1) were introduced to account for uncertainty. The standard deviation values were calculated from previous experimental data and tabulated uncertainty values. The parameter uncertainty-sensitive optimization results are depicted in Fig. 2.

Table 1. Standard deviations of parameters and design variables formerly assumed to be deterministic.

Parameter/ Design variable	Standard Deviation
ν	0.1
x	0.001 mm
V_f	0.005
L_2	0.001 mm
L_3	0.001 mm

In order to analyze the robustness of the objective with a Monte Carlo simulation, a convergence study was performed to find a minimum number of random simulation points that could repeatedly converge to an optimal change in resistance. Fig. 2 shows that $5x10^5$ simulation points is sufficient to converge using the reported uncertainties. The simulation produced the histogram in Fig. 3 which shows that the uncertainty in the material properties and dimensions leads to a distribution that is heavily one sided. Referring to Eq. 5, one can see that the majority of the terms with uncertainty are squared and this causes small variations due to uncertainty to greatly increase the objective value. Even though the mean of this simulation was close to 25 kOhm/ϵ, the greatest value is well over 6 times the mean. However, the tail of this distribution is extremely small, less than 1% of the simulations lie above 100 kΩ/ϵ.

C. Transmitted Variance

Strictly following the deterministic optimization results, strain gauges should be manufactured at the brink of their usability to reach their optimum change in resistance. In reality, since there is inherent variability in the manufacturing process, this would produce roughly half of the strain gauges violating each constraint. With three constraints, this configuration would produce strain gauges that are 12.5% reliable (0.5^3). In order to account for this variation in the manufacturing process, the simple transmitted variance method was used to find the 97% reliable optimum (0.99^3) strain gauge configuration (Fig. 4). This reliable optimum produces strain gauges with lower objective values than the deterministic, but in practice performs much better in response to uncertainty. With this design, the cost to manufacture can be decreased and the ease of manufacturing can be increased. The repeatability of both solutions will be the same: the variance in the design variables does not have an impact on the robustness of our solution.

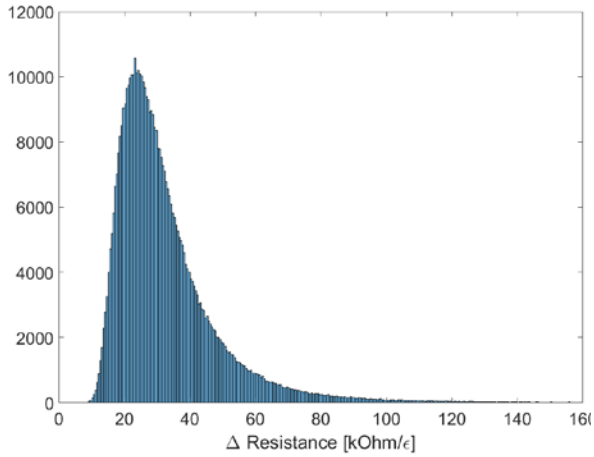

Figure 3. Histogram of Monte Carlo objective value results at ϵ = 0.15 with $5x10^5$ simulations.

IV. Conclusions

At every strain level, design variables were found to be yield optimal resistance when right on the constraints. Sensor width and thickness give the best performance when they are on the limit of being too small to be manufactured (5 and 1 mm, respectively). Similarly, the filler volume fraction produces the best resistance range when it is the highest allowable by current manufacturing methods. These agree with engineering intuition and Eq 5; more conductive filler in a composite with a smaller cross-section yields a higher possible range of electrical resistance. Looking at the objective values at the optimized sensor configuration shows that sensors perform best at lower induced strains. Strains above 15% yield a change of resistance in ranges less than 100 Ω, which produces changes in voltage below the acceptable resolution of most commercial voltage sensors. As such, under the specified configuration, these composite sensors should not be relied upon to give accurate signals above 10% strain.

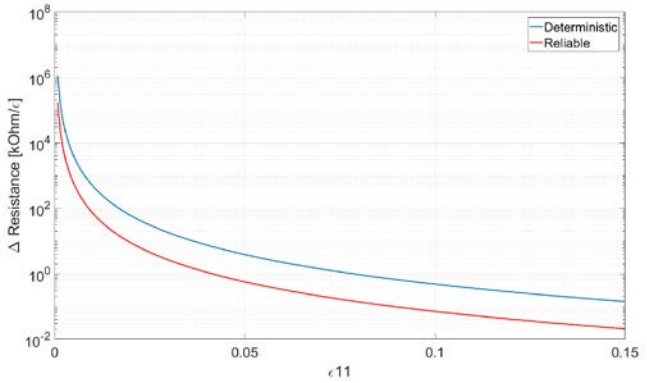

Figure 3: Deterministic (12.5% reliable) versus 97% reliable objective function values for strains of 0.01-0.15.

References

1. Wang, Q.-M., et al., *Electromechanical coupling and output efficiency of piezoelectric bending actuators.* IEEE transactions on ultrasonics, ferroelectrics, and frequency control, 1999. **46**(3): p. 638-646.
2. Liang, C., F. Sun, and C.A. Rogers, *Electro-mechanical impedance modeling of active material systems.* Smart Materials and Structures, 1996. **5**(2): p. 171.
3. Wissler, M. and E. Mazza, *Electromechanical coupling in dielectric elastomer actuators.* Sensors and Actuators A: Physical, 2007. **138**(2): p. 384-393.
4. Hogan, N. *Impedance control: An approach to manipulation.* in *American Control Conference, 1984*. 1984. IEEE.
5. Witt, G., *The electromechanical properties of thin films and the thin film strain gauge.* Thin Solid Films, 1974. **22**(2): p. 133-156.
6. Stutts, D. *A simple example of the relationship between electromechanical coupling and measured impedance*. 1995; Available from: http://web.mst.edu/~piezo/MotorAnalysis/Impedancemodel/Imped-Mo.html.